

Status of the Experimental Studies on DVMP and Transversity GPDs

Valery Kubarovsky*

and the CLAS collaboration

Thomas Jefferson National Accelerator Facility

Newport News, VA 23606, USA

E-mail: vpk@jlab.org

The cross section of the exclusive π^0 and η electroproduction reaction $ep \rightarrow e'p'\pi^0/\eta$ was measured at Jefferson Lab with a 5.75-GeV electron beam and the CLAS detector. Differential cross sections $d^4\sigma/dtdQ^2dx_Bd\phi$ and structure functions $\sigma_U = \sigma_T + \varepsilon\sigma_L, \sigma_{TT}$ and σ_{LT} , as functions of t were obtained over a wide range of Q^2 and x_B . At low t , both π^0 and η are described reasonably well by Generalized Parton Distributions (GPDs) model in which chiral-odd transversity GPDs are dominant. Generalized form factors of the transversity GPDs $\langle H_T \rangle^{\pi,\eta}$ and $\langle \bar{E}_T \rangle^{\pi,\eta}$ were directly extracted from the experimental observables. The combined π^0 and η data opens the way for the flavor decomposition of the transversity GPDs. The first ever demonstration of this decomposition was done for the transversity GPDs H_T and \bar{E}_T . GPD \bar{E}_T is connected with the density of the polarized quarks in an unpolarized nucleon in the impact parameter space. The spin density of polarized u and d -quarks was evaluated for different values of Feynman x from the GPD model tuned to described the experimental data.

*23rd International Spin Physics Symposium - SPIN2018 -
10-14 September, 2018
Ferrara, Italy*

*Speaker.

1. Introduction

Understanding nucleon structure in terms of the fundamental degrees of freedom of Quantum Chromodynamics (QCD) is one of the main goals in the theory of strong interactions. In recent years it became clear that exclusive reactions may provide information about hadron structure encoded in so-called Generalized Parton Distributions [1, 2] (GPDs). For each quark flavor q there are eight GPDs. Four correspond to parton helicity-conserving (chiral-even) processes, denoted by H^q , \tilde{H}^q , E^q and \tilde{E}^q , and four correspond to parton helicity-flip (chiral-odd) processes [3, 4], H_T^q , \tilde{H}_T^q , E_T^q and \tilde{E}_T^q . The GPDs depend on three kinematic variables: x , ξ and t . In a symmetric frame, x is the average longitudinal momentum fraction of the struck parton before and after the hard interaction and ξ (skewness) is half of the longitudinal momentum fraction transferred to the struck parton. The skewness can be expressed in terms of the Bjorken variable x_B as $\xi \simeq x_B/(2 - x_B)$. Here $x_B = Q^2/(2p \cdot q)$ and $t = (p - p')^2$, where p and p' are the initial and final four-momenta of the nucleon.

When the theoretical calculations for longitudinal virtual photons were compared with the JLab π^0 and η data [5, 6, 7] they were found to underestimate the measured cross sections by more than an order of magnitude in their accessible kinematic regions. The failure to describe the experimental results with quark helicity-conserving operators stimulated a consideration of the role of the chiral-odd quark helicity-flip processes. Deeply virtual meson electroproduction (DVMP), and in particular π^0 production in the reaction $ep \rightarrow e'p'\pi^0$, was identified [8, 9, 10] as especially sensitive to the quark helicity-flip subprocesses. During the past few years, two parallel theoretical approaches - [8, 11] (GL) and [9, 10] (GK) have been developed utilizing the chiral-odd GPDs in the calculation of pseudoscalar meson electroproduction. The GL and GK approaches, though employing different models of GPDs, lead to *transverse* photon amplitudes that are much larger than the longitudinal amplitudes.

2. Definition of structure functions

The unpolarized reduced meson cross section is described by 4 structure functions σ_T , σ_L , σ_{TT} and σ_{LT} :

$$2\pi \frac{d^2\sigma(\gamma^* p \rightarrow p\pi^0)}{dt d\phi} = \frac{d\sigma_T}{dt} + \varepsilon \frac{d\sigma_L}{dt} + \varepsilon \frac{d\sigma_{TT}}{dt} \cos 2\phi + \sqrt{2\varepsilon(1+\varepsilon)} \frac{d\sigma_{LT}}{dt} \cos \phi. \quad (2.1)$$

References [10, 11] obtain the following relations for unpolarized structure functions:

$$\frac{d\sigma_L}{dt} = \frac{4\pi\alpha}{k'} \frac{1}{Q^4} \left\{ (1 - \xi^2) |\langle \tilde{H} \rangle|^2 - 2\xi^2 \text{Re} [\langle \tilde{H} \rangle^* \langle \tilde{E} \rangle] - \frac{t'}{4m^2} \xi^2 |\langle \tilde{E} \rangle|^2 \right\} \quad (2.2)$$

$$\frac{d\sigma_T}{dt} = \frac{4\pi\alpha}{2k'Q^4} \left[(1 - \xi^2) |\langle H_T \rangle|^2 - \frac{t'}{8m^2} |\langle \bar{E}_T \rangle|^2 \right] \quad (2.3)$$

$$\frac{d\sigma_{LT}}{dt} = \frac{4\pi\alpha}{\sqrt{2}k'Q^4} \xi \sqrt{1 - \xi^2} \frac{\sqrt{-t'}}{2m} \text{Re} [\langle H_T \rangle^* \langle \tilde{E} \rangle] \quad (2.4)$$

$$\frac{d\sigma_{TT}}{dt} = \frac{4\pi\alpha}{k'Q^4} \frac{t'}{16m^2} |\langle \bar{E}_T \rangle|^2 \quad (2.5)$$

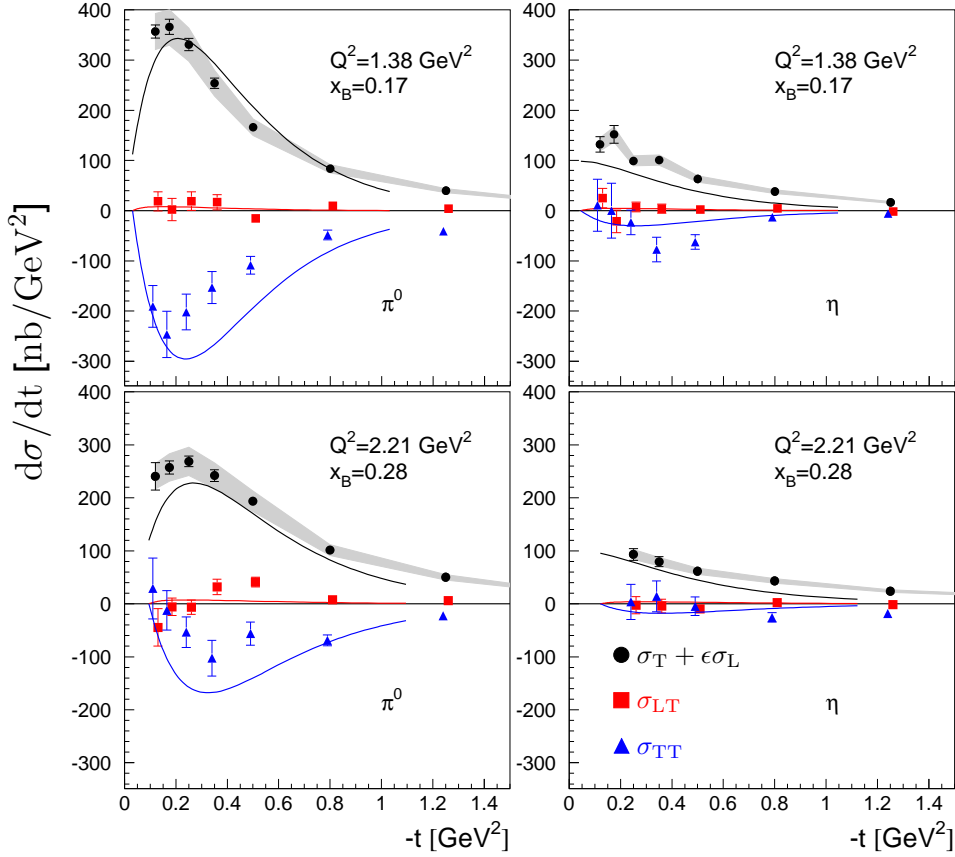


Figure 1: (Color online) The extracted structure functions vs. t for the π^0 (left column) and η (right column). The top row presents data for the kinematic point ($Q^2 = 1.38 \text{ GeV}^2$, $x_B = 0.17$) and bottom row for the kinematic point ($Q^2 = 2.21 \text{ GeV}^2$, $x_B = 0.28$). The data and curves are as follows: black circles - $d\sigma_U/dt = d\sigma_T/dt + \epsilon d\sigma_L/dt$, blue triangles - $d\sigma_{TT}/dt$, red squares - $d\sigma_{LT}/dt$. The error bars are statistical only. The gray bands are our estimates of the absolute normalization systematic uncertainties on $d\sigma_U/dt$. The curves are theoretical predictions produced with the GPG model of Goloskokov and Kroll [10].

Here m is the mass of the proton, $t' = t - t_{min}$, where $|t_{min}|$ is the minimum value of $|t|$ corresponding to $\theta_\pi = 0$, $k'(Q^2, x_B)$ is a phase space factor and $\bar{E}_T = 2\tilde{H}_T + E_T$. The brackets $\langle H_T \rangle$ and $\langle \bar{E}_T \rangle$ denote the convolution of the elementary process $\gamma^* q \rightarrow q\pi^0$ with the GPDs H_T and \bar{E}_T . They are called them generalized form factors.

3. Experimental data

The cross section of the reaction $ep \rightarrow ep(\pi^0/\eta)$ measured by the CLAS collaboration at Jlab in bins of Q^2 , x_B , t and ϕ were published in Refs. [5, 6, 7]. Structure functions $\sigma_U = \sigma_T + \epsilon\sigma_L$, σ_{LT} and σ_{TT} have been extracted from the angular distributions. These functions were compared with the predictions of the GPD models [10, 11]. The result confirmed that the measured unseparated cross sections are much larger than expected from leading-twist handbag calculations which are dominated by longitudinal photons. As an example, the comparison of the π^0 and η structure

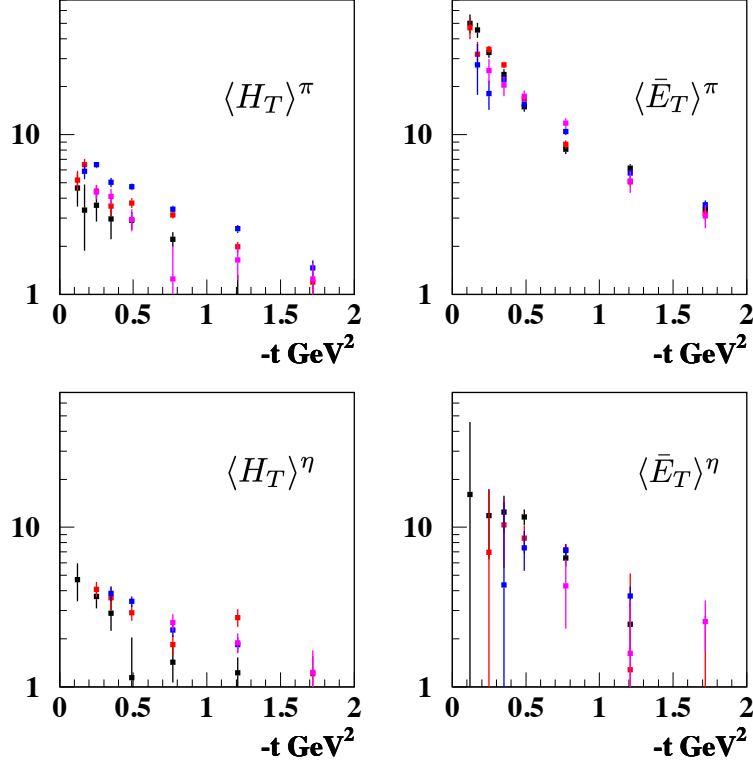


Figure 2: (Color online) Data points: CLAS. Top left: $|\langle H_T \rangle^\pi|$, top right: $|\langle \bar{E}_T \rangle^\pi|$, bottom left: $|\langle H_T \rangle^\eta|$, bottom right: $|\langle \bar{E}_T \rangle^\eta|$ as a function of $-t$ for different kinematics: ($Q^2=1.2 \text{ GeV}^2$, $x_B=0.15$) black, ($Q^2=1.8 \text{ GeV}^2$, $x_B=0.22$) red, ($Q^2=2.2 \text{ GeV}^2$, $x_B=0.29$) blue, ($Q^2=2.7 \text{ GeV}^2$, $x_B=0.34$) magenta.

functions is shown in Fig. 1 for two kinematical bins in x_B and Q^2 . The structure functions σ_U and σ_{TT} for η are, respectively, factors of 2.5 and 10 smaller than for π^0 . However, the GK GPD model [10] (curves) follows the experimental data. Taken together, the π^0 and η results strengthen the statement about the transversity GPD dominance in the pseudoscalar electroproduction process.

4. Generalized form factors

The squared magnitudes of the generalized form factors $|\langle H_T \rangle|^2$ and $|\langle \bar{E}_T \rangle|^2$ may be directly extracted from the experimental data (see Eqs. 2.3 and 2.5) in the framework of GPD models.

$$|\langle \bar{E}_T \rangle^{\pi,\eta}|^2 = \frac{k' Q^4}{4\pi\alpha} \frac{16m^2}{t'} \frac{d\sigma_{TT}^{\pi,\eta}}{dt} \quad (4.1)$$

$$|\langle H_T \rangle^{\pi,\eta}|^2 = \frac{2k' Q^4}{4\pi\alpha} \frac{1}{1-\xi^2} \left[\frac{d\sigma_T^{\pi,\eta}}{dt} + \frac{d\sigma_{TT}^{\pi,\eta}}{dt} \right]. \quad (4.2)$$

Figure 2 presents the modulus of the generalized form factors $|\langle H_T \rangle^\pi|$, $|\langle \bar{E}_T \rangle^\pi|$, $|\langle H_T \rangle^\eta|$ and $|\langle \bar{E}_T \rangle^\eta|$ for 4 different kinematics. Note the dominance of the $|\langle \bar{E}_T \rangle|$ over $|\langle H_T \rangle|$ for both π^0 and η . Generalized form factors $\langle H_T \rangle^\pi$ and $\langle \bar{E}_T \rangle^\pi$ are shown in more detail in Fig. 3. The $\langle \bar{E}_T \rangle^\pi$ formfactor

has steeper t-dependence than $\langle H_T \rangle^\pi$. The t-slope parameters, obtained by an exponential fit of the form e^{bt} , are $b(\langle \bar{E}_T \rangle) = 1.27 \text{ GeV}^{-2}$ and $b(\langle H_T \rangle) = 0.98 \text{ GeV}^{-2}$.

5. Flavor decomposition

In electroproduction of π^0 and η mesons the GPDs F_i appears in the following combinations

$$F_i^\pi = \frac{1}{\sqrt{2}} [e_u F_i^u - e_d F_i^d] \quad (5.1)$$

$$F_i^\eta = \frac{1}{\sqrt{6}} [e_u F_i^u + e_d F_i^d - 2e_s F_i^s] \quad (5.2)$$

The q and \bar{q} GPDs contribute in the quark combinations $F_i^q - F_i^{\bar{q}}$. Hence there is no contribution from the strange quarks if we assume that $F_i^s \simeq F_i^{\bar{s}}$. For flavor decomposition we have to take into account the decay constants f_π and f_η , the chiral condensate constants $\mu_{\pi^0} = 2.57 \text{ GeV}$, $\mu_1 = 0.958 \text{ GeV}$ and $\mu_8 = 2.32 \text{ GeV}$, and the contribution from singlet and octet η states [10].

$$F_i^\eta = F_i^\pi \left(\cos \theta_8 - \sqrt{2} \frac{\mu_1 f_1}{\mu_8 f_8} \sin \theta_1 \right) \frac{f_8 \mu_8}{f_{\pi^0} \mu_{\pi^0}} = \frac{F_i^8}{k_\eta}, \quad (5.3)$$

where the mixing angles are: $\theta_8 = -21.2^\circ$ and $\theta_1 = -9.2^\circ$. The octet and singlet wave functions are very similar and the decay constants are close as well $f_8 = 1.26 f_\pi$ and $f_1 = 1.17 f_\pi$. The overall factor for the η meson is $k_\eta = 0.863$. Using $e_u = \frac{2}{3}$ and $e_d = -\frac{1}{3}$ we will end up with

$$F_i^\pi = \frac{1}{3\sqrt{2}} [2F_i^u + F_i^d] \quad (5.4)$$

$$k_\eta F_i^\eta = \frac{1}{3\sqrt{6}} [2F_i^u - F_i^d]. \quad (5.5)$$

Experimentally we have access only to the $|\langle F_i^\pi \rangle|^2$ and $|\langle F_i^\eta \rangle|^2$ (see Eq. 4.1-4.2). The final equation for the $\langle H_T \rangle$ convolution reads

$$\frac{1}{18} |2\langle H_T \rangle^u + \langle H_T \rangle^d|^2 = |\langle H_T \rangle^\pi|^2 \quad (5.6)$$

$$\frac{1}{54} |2\langle H_T \rangle^u - \langle H_T \rangle^d|^2 = k_\eta^2 |\langle H_T \rangle^\eta|^2. \quad (5.7)$$

and similar equations for $\langle \bar{E}_T \rangle$.

The solution of these equations will lead to the flavor decomposition of the generalized form factors $\langle H_T \rangle^u$ and $\langle H_T \rangle^d$ as well as $\langle \bar{E}_T \rangle^u$ and $\langle \bar{E}_T \rangle^d$. However, the convolution integrals have real and imaginary parts. So it is impossible to solve these equations unambiguously with only two equations in hands. So, in order to estimate the form factors, we make an ad hoc assumption that the relative phase $\Delta\phi$ between $\langle H_T \rangle^u$ and $\langle H_T \rangle^d$ equals 0 or 180 degrees. Ignoring an overall phase, the form factors are then real, and we arbitrarily choose the solution with $\langle H_T \rangle^u$ and $\langle \bar{E}_T \rangle^u$ positive. Fig. 4 presents $\langle H_T \rangle^u$, $\langle H_T \rangle^d$, $\langle \bar{E}_T \rangle^u$ and $\langle \bar{E}_T \rangle^d$ for one kinematic point ($Q^2 = 2.2 \text{ GeV}^2, x_B = 0.27$) calculated with this assumption. Note the different signs of $\langle H_T \rangle^u$ and $\langle H_T \rangle^d$ and the same sign of $\langle \bar{E}_T \rangle^u$ and $\langle \bar{E}_T \rangle^d$. The theoretical predictions of the large- N_c QCD model [12] are consistent with this spin-flavor structure extracted from hard exclusive π^0 and η electroproduction data.

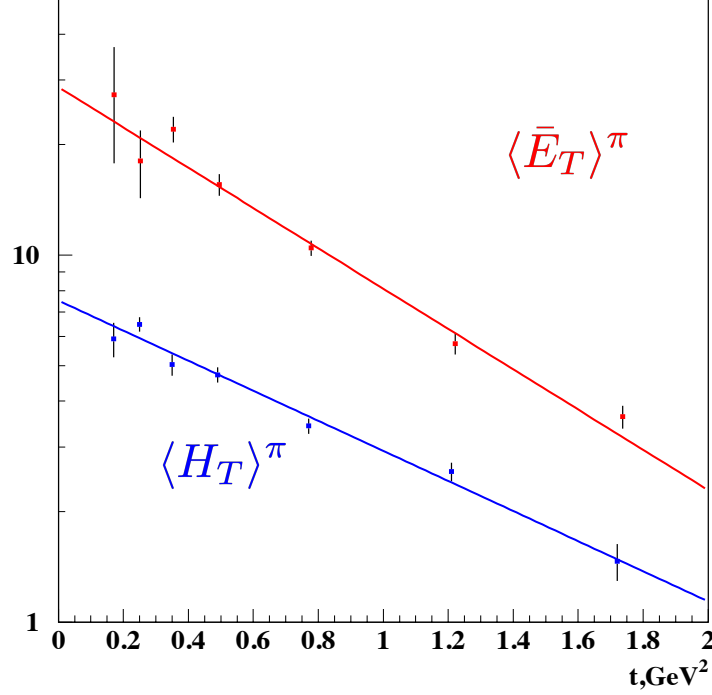


Figure 3: (Color online) Generalized form factors $|\langle H_T \rangle^\pi|$ and $|\langle \bar{E}_T \rangle^\pi|$ as a function of $-t$ for $Q^2 = 2.2 \text{ GeV}^2$ and $x_B = 0.27$. Top: $|\langle \bar{E}_T \rangle^\pi|$ in red; Bottom: $|\langle H_T \rangle^\pi|$ in blue.

6. Quark spin densities in the transverse plane and generalized transversity distributions

Two-dimensional Fourier transforms of GPDs $H(x, \xi = 0, -\vec{\Delta}^2)$ and $\bar{E}_T(x, 0, -\vec{\Delta}^2)$, where $\vec{\Delta}^2 = -t$, define the spin density of the polarized quarks in an unpolarized proton [13].

$$H(x, \vec{b}) = \int \frac{d^2 \vec{\Delta}}{(2\pi)^2} e^{-i\vec{b}\vec{\Delta}} H(x, 0, -\vec{\Delta}^2) \quad (6.1)$$

$$\bar{E}_T(x, \vec{b}) = \int \frac{d^2 \vec{\Delta}}{(2\pi)^2} e^{-i\vec{b}\vec{\Delta}} \bar{E}_T(x, 0, -\vec{\Delta}^2) \quad (6.2)$$

The GPDs $\bar{E}_T(x, \xi = 0, t)$ and $H(x, \xi = 0, t)$ were parametrized in the form [14]

$$\bar{F}^q(x, \xi = 0, t) = g^q(x) \cdot \exp[(f^q(x)t)],$$

where $g^q(x)$ and $f^q(x)$ are the GPD forward limit and profile functions respectively. The Fourier transform for this parametrization reads

$$\bar{F}^q(x, b) = \frac{1}{4\pi} \frac{g^q(x)}{f^q(x)} \exp\left[\frac{-b^2}{4f^q(x)}\right]. \quad (6.3)$$

For quarks polarized along b_x -axis the impact parameter density reads [13]

$$\delta^q(x, \vec{b}) = \frac{1}{2} \left[H^q(x, \vec{b}) - \frac{b_y}{m} \frac{\partial}{\partial b^2} \bar{E}_T^q(x, \vec{b}) \right]. \quad (6.4)$$

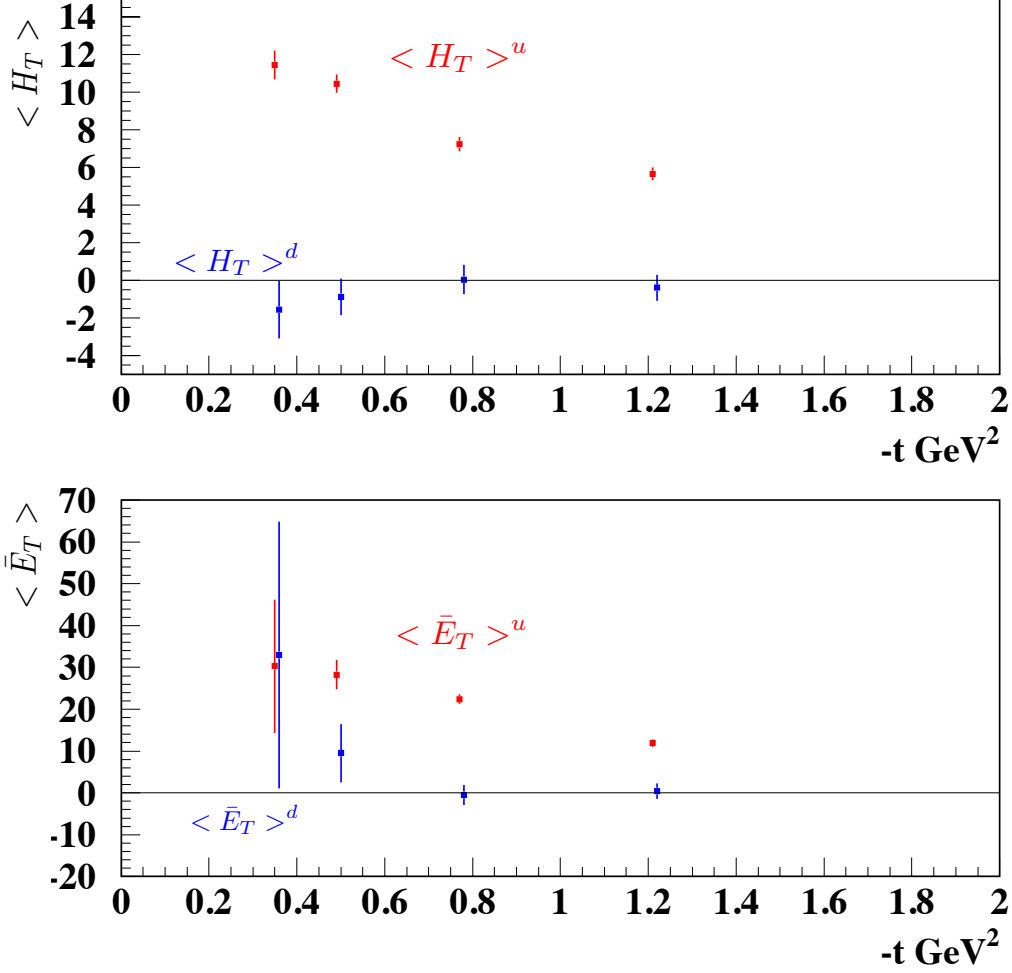


Figure 4: (Color online) Flavor separated generalized form factors $\langle H_T \rangle$ and $\langle \bar{E}_T \rangle$ as a function of $-t$ for $Q^2 = 2.2 \text{ GeV}^2$ and $x_B=0.27$. Top: $\langle H_T \rangle^u$ (red) and $\langle H_T \rangle^d$ (blue); Bottom: $\langle \bar{E}_T \rangle^u$ (red) and $\langle \bar{E}_T \rangle^d$ (blue).

The GPD $H(x, \vec{b})$ describes the density of unpolarized quarks and $\bar{E}_T(x, \vec{b})$ is related to the distortion of the polarized quark distribution in the transverse plane. We can map the u and d -quark transverse spin density distributions as a function of Feynman x based on the GPD model [10] tuned to describe the CLAS data. For example, Fig. 5 shows the impact parameter density of transversely polarized quarks along the b_x -axis in an unpolarized proton for Feynman $x=0.1$ and $x=0.2$. Note the distortion along b_y -axis, similar for u and d -quarks. Looking at the transverse quark density distribution, we can say that this width is diminished as $x \rightarrow 1$. This behavior is typical for the GPD models.

Polarized Quarks in Unpolarized Proton

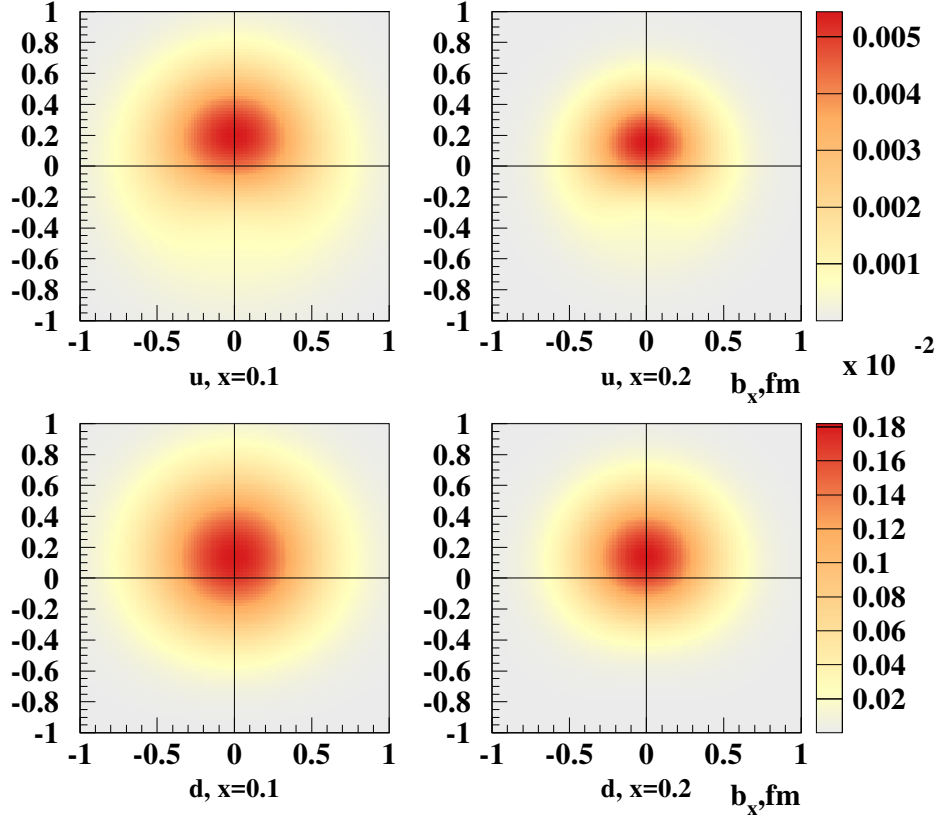


Figure 5: (Color online) Impact parameter density of quarks which are transversely polarized along b_x -axis in an unpolarized proton. Top left and right panels are for u-quarks with $x=0.1$ and $x=0.2$, respectively. Bottom left and right panels are for d-quarks with $x=0.1$ and $x=0.2$.

7. Conclusion

Differential cross sections of exclusive π^0 and η electroproduction have been obtained in the few-GeV region at more than 1800 kinematic points in bins of Q^2, x_B, t and ϕ_π . Virtual photon structure functions σ_U, σ_{TT} and $d\sigma_{LT}$ have been obtained. It is found that σ_U and σ_{TT} are comparable in magnitude with each other, while σ_{LT} is very much smaller than either. Generalized form factors of the transversity GPDs $\langle H_T \rangle^{\pi, \eta}$ and $\langle \bar{E}_T \rangle^{\pi, \eta}$ were directly extracted from the experimental observables for the first time. It was found that the GPD \bar{E}_T dominates in pseudoscalar meson production. The combined π^0 and η data opens the way for the flavor decomposition of the transversity GPDs. Within some simplifying assumptions, the decomposition has been demonstrated. The spin density of polarized u and d -quarks in the transverse plane was evaluated for different values of x from the GPD model tuned to describe the experimental data.

Acknowledgments

The author thanks G. Goldstein, S. Goloskokov, P. Kroll, S. Liuti, A. Radyushkin, P. Schweitzer

and C. Weiss for many informative discussions and making available the results of their calculations. This material is based upon work supported by the U.S. Department of Energy, Office of Science, Office of Nuclear Physics under contract DE-AC05-06OR23177.

References

- [1] X. Ji, *Phys. Rev. Lett.* **78**, 610 (1997); *Phys. Rev. D* **55**, 7114 (1997).
- [2] A.V. Radyushkin, *Phys. Lett. B* **380**, 417 (1996); *Phys. Rev. D* **56**, 5524 (1997).
- [3] P. Hoodbhoy and X. Ji, *Phys. Rev. D* **58**, 054006 (1998).
- [4] M. Diehl, *Phys. Rep.* **388**, 41 (2003) and references within.
- [5] I. Bedlinskiy *et al.* (CLAS Collaboration), *Phys. Rev. Lett.* **109**, 112001 (2012).
- [6] I. Bedlinskiy *et al.* (CLAS Collaboration), *Phys. Rev. C* **90**, 025205 (2014).
- [7] I. Bedlinskiy *et al.* (CLAS Collaboration), *Phys. Rev. C* **95**, 035202 (2017).
- [8] S. Ahmad, G. R. Goldstein and S. Liuti, *Phys. Rev. D* **79**, 054014 (2009).
- [9] S. V. Goloskokov and P. Kroll, *Eur. Phys. J. C* **65**, 137 (2010).
- [10] S. V. Goloskokov and P. Kroll, *Eur. Phys. J. A* **47**, 112 (2011).
- [11] G. Goldstein, J. O. Gonzalez-Hernandez and S. Liuti, *Phys. Rev. D* **84**, 034007 (2011); *Int. J. Mod. Phys. Conf. Ser.* **20**, 222 (2012); *J. Phys. G: Nucl. Part. Phys.* **39** 115001 (2012).
- [12] P. Schweitzer and C. Weiss, *Phys. Rev. C* **94**, 045202 (2016).
- [13] M. Diehl and Ph. Hagler, *Eur. Phys. J. C* **44**, 87 (2005).
- [14] M. Diehl and P. Kroll, *Eur. Phys. J. C* **73**, 2397 (2013).